INKJET DEPOSITION SYSTEM WITH COMPUTER VISION-BASED CALIBRATION FOR TARGETING ACCURACY

Lee E. Weiss, Larry Schultz, Eric Miller
Carnegie Mellon University
lew@cs.cmu.edu

CMU-RI-TR-06-15

March 2006

Abstract

This report describes a custom inkjet system, which was developed at the Robotics Institute, for accurately depositing various material inks onto or relative to specified target locations on substrates. The system uses computer vision-based calibration to achieve targeting accuracies of 4 μm or less with drop-on-demand inkjets. This versatile system is currently used for several diverse research programs at Carnegie Mellon, ranging from gas chemical sensor manufacturing to biological patterning. For example, chemically-sensitive semi-conducting polymers are deposited onto arrays of CMOS-MEMS and FET microtransducers in order to fabricate chemical sensor microarrays. These sensors are being integrated into multi-modal systems that combine different sensing modalities with different polymers on a single chip. For another example, bioinks of growth factors are deposited onto biological substrates to form patterned arrays of these factors. To precisely quantify cell responses relative to these patterns it is important print these patterns relative to specific locations on the substrates to facilitate subsequent registration in the cell culture imaging system.

INKJET DEPOSITION SYSTEM
WITH COMPUTER VISION-BASED CALIBRATION
FOR TARGETING ACCURACY

Lee E. Weiss
Larry Schultz
Eric Miller

INTRODUCTION

This technical report describes a custom inkjet system used to accurately deposit various material inks onto or relative to specified target locations on substrates. This versatile system is currently used for several diverse research programs at Carnegie Mellon, ranging from gas chemical sensor manufacturing to biological patterning.

Gas Chemical Sensors: In this project, chemically-sensitive polymers are deposited onto arrays of microtransducers in order to fabricate gas chemical sensor microarrays by coupling semiconducting chemically-sensitive regio-regular polymers with CMOS-MEMS and FET microtransducers[1]. These sensors are being integrated into multi-modal systems that combine different sensing modalities with different polymers on a single chip (eg. **Fig. 1**)

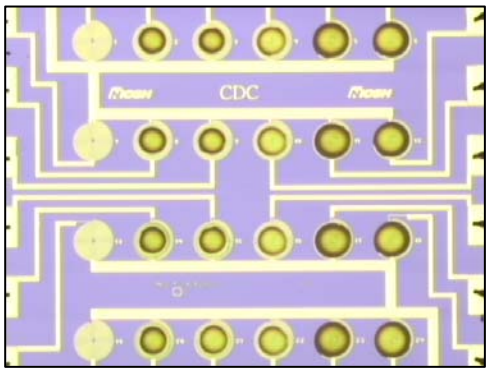

Figure 1. Gas chemical sensor ('electronic nose') fabricated by inkjetting multiple chemically sensitive polymers on array of spiral electrodes

Fabricating these multi-modal sensors requires a process that can selectively, accurately, and repeatably deposit picoliter quantities of polymers dissolved in organic solvents onto the microtransducers. There are numerous processes to consider for organic electronic manufacturing applications requiring selective deposition of semiconductor polymers.[2, 3] The specific requirements for the sensors we are developing include: a non-contact deposition process to accommodate MEMS and other non-planar structures; a quick fabrication turn-around time to be able to quickly prototype new ideas and to screen the wide variety of candidate polymers being synthesized; compatibility with small research stocks (milligrams) of polymers; and, a process that deposits polymers from the liquid-phase to allow sufficient time for the semi-conducting polymers to self-assemble into nanowires. Inkjet deposition satisfies these requirements. It is a versatile, cost-effective, and programmable approach that has been used for a range of organic electronic manufacturing applications, including organic thin-film transistors, organic light-emitting diodes, photovoltaic grids, and other sensors.[4-10]

The desired targeting accuracy for depositing onto our sensor arrays is approximately 5 μm. With this level of precision it is not practical to use mechanical fixturing to pre-align and register the chips relative to the inkjets since small deviations from nominal drop trajectories occur due

to nozzle-to-nozzle geometry variations and random wetting of the nozzles over time. Small variations in the mounting alignment of the jets also occur after an inkjet has been removed for cleaning and then remounted. Furthermore, small variations in the dimensions of diced prototype chips can be greater than 5 μm. A practical and easy-to-use deposition system therefore requires optical calibration to reliably achieve the desired targeting accuracy. This report presents a detailed description of our inkjet deposition system with computer vision-based calibration for targeting accuracy.

Biological Patterning: In another application, inkjet deposition is used to deposit concentration modulated patterns of growth factors onto biological substrates such as fibrin-coated glass slides[11, 12] (e.g., **Fig. 2**). The surface concentrations of the growth factors are modulated by overprinting with dilute bioinks. After the patterns are printed, they are transferred to an extended-time-lapse imaging/cell culture system in order to observe cell responses to these patterns. To precisely quantify cell responses relative to these patterns it is important to register the patterns to the image frame in the cell culture imaging system. While fluorescently-labeled bioinks could be used to visual the patterns, as in **Fig. 2**, we do not use labeled inks for the cell studies since the labeling affects cells responses. Therefore it is important to print relative to known, easily visualized locations on the glass slides, such as corners or edges. The same calibration methods used for sensor fabrication application can be used for this biological application.

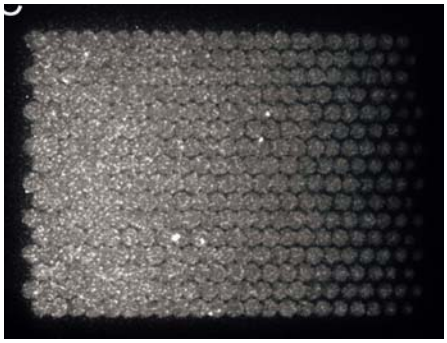

Figure 2. Concentration-modulated gradient of fluorescently-labeled FGF-2 printed on fibrin-coated glass slide

Overview of Deposition System

We built a custom inkjet deposition system (**Fig. 3**) that can deposit droplets onto specific target locations with an accuracy of 4 μm or less. Droplet sizes range from 18 pl for aqueous-based biological inks up to to 45 pl for the organic solvent-based polymer inks. A simplified schematic of the deposition system is shown in **Fig. 4**. The tip of the inkjet is positioned close above the target substrate, within 180 μm, to maximize jetting accuracy onto the targets. However, this arrangement prevents direct viewing of the jetted drops onto the transducers as a visual aid to targeting because the 560 μm diameter tip of the inkjet obscures the 200 μm targets (e.g., sensor

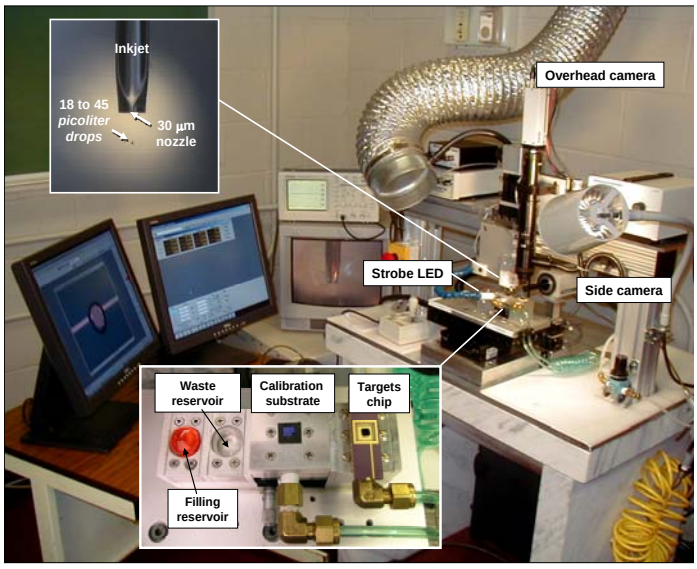

FIGURE 3: Inkjet deposition system.

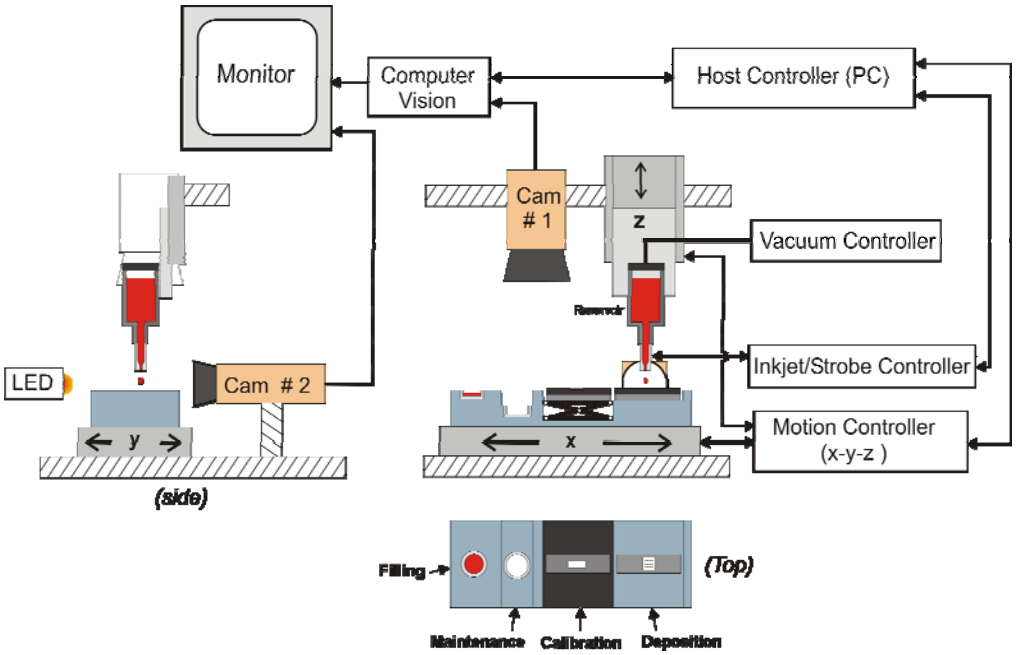

Figure 4. System integration.

electrodes or corner of glass slides). Therefore, the system incorporates a targeting calibration method using computer vision feedback from an overhead camera ('Cam #1') to measure the positional offset between the targeted transducer and test drops deposited onto a calibration substrate. This camera is also used to inspect deposited drop ('splat') morphologies. A strobe-illuminated side camera ('Cam #2') is used to image drops in-flight to provide visual feedback to the operator while he/she is adjusting the jetting parameters to achieve a stable jet.

The system is arranged into four workstations that are moved by X-Y servo stages relative to the fixed inkjet and overhead camera. The inkjet is mounted on a servo-controlled Z-stage to adjust the nozzle stand-off height relative to the workstations. The workstations include:

- ***Filling station*** where the inkjet is lowered into a small dish of ink, and a vacuum is pulled to fill the inkjet reservoir.
- ***Maintenance station*** where ink is jetted into a waste vessel while droplets in-flight, which are illuminated with strobe LED synced to the jetting pulses, can be observed by the operator.
- ***Calibration station*** where a vacuum chuck holds either a silicon dioxide wafer (for chemical sensor printing) or a fibrin-coated glass coverslip (for biological printing) onto which test drops are jetted are as part of the calibration procedure. The vacuum chuck is mounted on a miniature manually adjustable jack-stage which is used to adjust the height of the calibration substrate relative to the height of the sensor chip in the adjacent deposition station.
- ***Deposition station*** where the sensor chip arrays are placed onto another vacuum chuck and polymer drops are deposited onto the devices using calibration information for accurate drop placement.

MATERIALS AND METHOD DETAILS

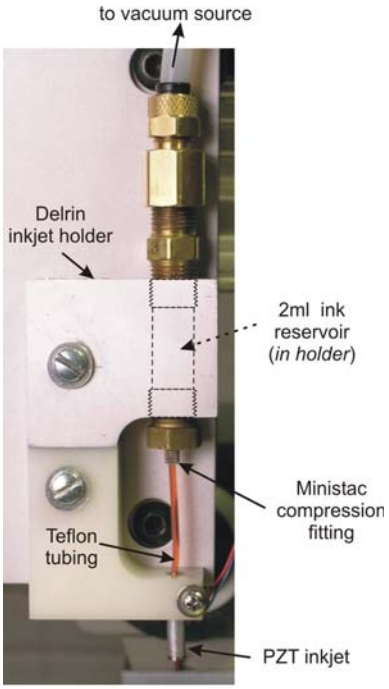

Figure 5. Inkjet holder and reservoir

InkJet. The system uses a commercially available drop-on-demand Microfab MJ-AB inkjet controlled with a JetDrive III controller (Microfab Technologies, Inc. Plano, TX). The inkjet consists of a glass tube, drawn down to a 30 μm nozzle, surrounded by and bonded to a tubular piezoelectric crystal. This inkjet is mounted in a custom holder with an integral reservoir under a vacuum which holds the ink in the capillary tube and maintains a meniscus at the nozzle when not jetting (**Fig. 5**). The vacuum is generated by a Venturi generator (SVC Ltd.Taiwan) and controlled using a digital regulator (J-Kem Scientific, Inc., St.Louis MO. Model 200). To jet a drop, the piezoelectric crytsal is actuated to apply a force to the fluid column to momentarily overcome the surface tension of the meniscus. An in-depth description of these types of inkjets and supporting technologies is presented by Lee[13].

Motion control components. The motion control system includes Aerotech ALS150 X-Y linear motor slides (+/- 0.3:m accuracy), ATS300 Z stage, and a Unidex 500 controller (Aerotech, Inc., Pgh. PA). Custom software performs high-level motion control and jetting coordination to implement the targeting and deposition strategies described below. A 40 mm miniature jack-stage (Edmund Optics Inc., Barrington, NJ) is used to adjust the height of the calibration substrate. The entire system is mounted on a marble table for stability, and an exhaust hood is incorporated since the inks are based on volatile organic solvents.

Computer vision compontents. Camera #1 is a Pulnix TMC-7DSP digital color video camera (Pulnix, Sunnyvale,CA), with a Navitar 12X zoom lens with coaxial illumination and a 2X adaptor (Navitar, Inc., Rochester, NY). Camera #2 is a monochrome CCD video camera with a standard 60 FPS RS-170A analog output (Panasonic Model WV-CL320, Panasonic Corp., Secaucus, NJ), and with an InfiniStix 44mm/1.50X lens (Infinity Photo-Optical Co., Boulder, CO). Both cameras are interfaced to a Matrox Orion asynchronous analog frame grabber controlled by Matrox imaging software (Matrox, Inc., Dorval, Quebec). The drops in-flight observed by Camera #2 are illuminated with an Everlight LED Super Bright (Everlight Electronic Co., LTD, Tu-Cheng City, China) driven by a strobe driver integral to the JetDrive III controller; the LED is attached to the end of a flexible gooseneck. Drops jetted at firing frequencies above 60 Hz can be easily observed in real time with the stroboscopic illumination triggered by the jet, but the jet rates that we use to deposit onto targets are typically .5Hz to 2Hz, which are relatively low. Observing drops jetted at these low rates would require a digital camera and frame grabber synchronously triggered by the jet/strobe signal to capture and display drop images. However, using a Phantom V7 high-speed motion capture system capable of capturing up to 160,000 frames/sec (Vision Research, Inc., Wayne, New Jersey), we have verified that drops jetted between .5 to 2 Hz using the same jetting parameters obtained by tuning the system at 100 to 300 Hz, look substantially the same in size and velocity as those tuned and jetted at 100

to 300 Hz. Therefore, to simplify system requirements, we tune jets at 100 HZ using the relatively inexpensive RS-170A camera and asynchronous frame grabber. We use the Phantom V7 in a separate jetting test bed for detailed observations of the various jetting processing used in our lab for this and other applications; this expensive high-speed camera is not intended for integration into a dedicated jetting system.

Ink Preparation

i. Polythiophene-based Inks for Sensor Fabrication: Inks are composed of polymers dissolved in highly volatile organic solvents including xylene, toluene, and 1,2,4-trichlorobenzne. All solvents are dried using 4A molecular sieve beads (4-8 mesh) (Sigma Aldrich, St. Louis, MO) prior to ink preparation. The beads are first prepared by drying in an oven at 250°C for 2 hours. The beads are cooled to ambient temperature under vacuum and then mixed with the solvents in an Erlenmeyer flask for 24 hours. The dried solvents are then used immediately. Typically, 4 ml quantities of ink are prepared for each jetting session. The inks are prepared by dispensing 4 ml of organic solvent into a mixing vial using a Fisher 4 ml glass volumetric pipette. The polymer granules are then weighed out using an Ohaus Adventurer SL AS64 analytical balance (Pinebrook, N.J) and then combined with the solvent. The mixtures are initially sonicated in a water bath using a Fisher Model FS-5 sonicator (Fisher Scientific Corp., Pittsburgh, PA) for approximately 20 minutes. After sonification the solution typically exhibits a dark opaque appearance which indicates that the polymer only partially dissolves in the solvent. The ink is then blended for 30 seconds using a Barnstead Maxi-Mixer (Barnstead International, Inc., Dubuque, Iowa). Afterwards, the mixture is gently heated in a water bath at 45°C for approximately 5 to 10 minutes depending on polymer type. The solvent mixture will have a transparent appearance when the polymer is almost fully dissolved in the solvent. After heating, the mixture is permitted to slowly cool to ambient temperature for 15 minutes. Low molecular weight polymers can sometimes be dissolved with only sonification.

The solution is then filtered to remove any undissolved polymer, contaminants, or debris using a series of progressive filtering steps. The solution is first prefiltered using 1.0 μm pore size Teflon syringe filters (Whatman Inc., Clifton, NJ). Afterwards, final filtering proceeds with 0.2 micron Teflon syringe filters (Whatman Inc., Clifton NJ). Low molecular weight polymers can be filtered using only a 0.2 μm filter while higher molecular weight polymers require progressive filtering. If the filtering steps of a higher molecular weight polymer are omitted, filter loading may occur.

ii. Bioinks. The bioink stock solutions are stored at -80°C and are thawed and diluted one hour before printing. The bioinks are diluted in buffers with a pH that is appropriate for that particular growth factor to a working concentration of between 1 and 100 μg/ml. The bioinks are maintained in sterile conditions and no filtering is performed prior to loading the inks in the inkjet.

Loading ink into the jet. The jet reservoir can be filled with ink either by loading ink into it from the top, or by drawing ink up into the reservoir from an ink-well in the filling station. We prefer to draw the ink into the reservoir by pulling vacuum because the 30 μm nozzle serves as a filter to prevent larger particles from entering the jet and clogging it.

The jet is positioned over the filling station, which holds a dish of ink, and the jet tip is lowered approximately 2 mm into the ink. Then ink is drawn up through the nozzle using negative pressure at 720 Torr. After approximately 75 microliters of ink has been loaded, the jet is raised out of the dish of ink and the meniscus is adjusted to be even with the tip of the nozzle using the vacuum regulator, using Camera #2 to observe the meniscus. The inkjet is reloaded when the fluid meniscus is visible in the Teflon tubing.

Tuning the Jetting Parameters. The control signal sequence **(Fig. 6**) to the piezoelectric crystal to produce a drop is:

i. Apply a positive-going voltage to expand the tube and draw fluid into the tube from the reservoir,
ii. Dwell to allow the pressure wave to propagate,
iii. Apply a negative-going voltage to compress the tube and squeeze fluid out of the nozzle, and
iv. Apply a negative voltage pulse to dampen resonances in the tube/ink.
v. Multiple drops are required to build up sufficient polymer to form each sensor, and thus the number of drops and the drop rate are also control parameters.

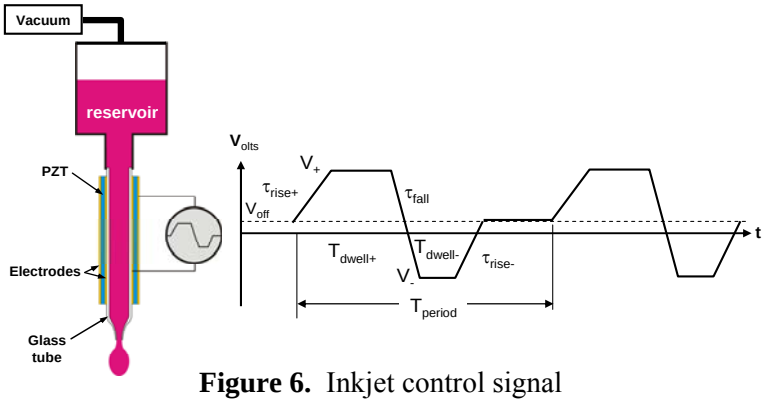

Figure 6. Inkjet control signal

To tune the jet, the system operator manually adjusts eight control signal parameters (through the MicroJet user interface) and the vacuum level by observing the drop responses using the side-camera (see insert in **Fig. 3**). Ideally, the parameters should be adjusted to produce a stable mono-disperse stream (single drop-per-trigger) which exhibits: no satellite drops; the smallest droplet size; maximum droplet velocity; minimum deviation from a straight-line trajectory; and, minimum velocity deviations from drop-to-drop. In addition, the parameters should produce a robust process such that variations in the inks, the jetting devices, or reservoir fluid level have minimal affects on jetting. Achieving optimization of droplet formation is challenging because of the large number of control parameters, the complex fluid rheology of the inks, and the high volatility of the solvents. While there have been efforts to use predictive modeling to help design inkjet devices[14, 15], these processes are in general difficult to model in a way that can predict and "in practice … settings …..are found by trial-and-error", however, there are rules that are useful for searching the space of parameters.[13, 16] Once successful parameters for a solvent/polymer combination have been established, only fine tuning may be required for using the same combination in subsequent jetting sessions.

Adjusting jet height relative to chip. The nominal stand-off height between the jet and the substrate is set to approximately 180 μm. The stand-off is adjusted by moving the jet with the servo Z-axis under joystick control while observing the tip relative to the substrate with the side

camera (Cam #2). Calibrated reticule marks are superimposed on the monitor as a visual aid to set the correct distance.

The nominal stand-off height is a trade-off between jetting accuracy and ability to observe jetting during normal operations. At 180 μm, we can still observe drops impinging on the substrates with the side camera to help verify that jetting is proceeding properly, but at shorter heights this becomes difficult. On the other hand, as the standoff-height increases, then jetting accuracy decreases.

Adjustment of chip and calibration substrate heights. Prior to performing the image-based targeting calibration, it is critical that the surfaces of the target chip and calibration substrate be at the same height. To accomplish this, the target chip is first moved under the overhead camera (Cam #1) at 21X lens magnification (725X system magnification), where the depth of field is 20 μm at this magnification, and then the lens is adjusted to bring an arbitrary device on this chip into focus. Next, the calibration chip (diced silicon dioxide wafer or fibrin-coated glass slide), which is mounted on the manual z-jack stage, is moved under Cam #1 and the z-stage height is adjusted until the chip's surface comes into focus. With this procedure, the top surfaces of chip and calibration substrates will be within 30 μm of each other.

Targeting Calibration. The targeting calibration procedure uses computer vision to determine the positional offset between targeted transducers (or glass slides) and test drops deposited onto a calibration substrate. Using transducer targeting as an example, the basic strategy is:

i. Jet a test drop onto the calibration substrate and record the x-y table positions (x_{cal}, y_{cal}) at that location,
ii. Move the calibration splat and target under the overhead camera, at a position in which they are both visible, and measure the x-y offset distances (Δx, Δy) between the center of the calibration splat and the center of the target (using a known camera pixel/distance factor), and
iii. Move the tables to ($x_{cal}+ \Delta x$, $y_{cal} + \Delta y$), which will align the target with subsequent jetted drops.

However, using this strategy to directly measure the offset is not practical because visualizing both the calibration splat and target in a single image requires low magnification, thus reducing resolution and targeting accuracy. Therefore, to achieve the highest resolution we use a strategy in which the calibration splat and the target are imaged separately under high magnification (21X lens, 725X system) while the positions of the X-Y servo stages at each location are recorded to determine the offset. The specific sequence is:

I. Jet a test drop anywhere onto the calibration substrate and record the X-Y table positions (x_{jet}, y_{jet}) at that location (**Fig. 7a**),
II. Move the calibration splat under the camera; find the splat's center-of-mass (COM_{cal}) in the camera's coordinate frame; draw a static cross-hair graphic through the COM; and, record the table position (x_{cal}, y_{cal}) (**Fig. 7b**),
III. Move the target transducer under camera so that the center of the target is aligned with the COM_{cal}, and record the table position (x_{target}, y_{target}) (**Fig. 7c**), and

IV. Move the tables to (x_{jet}+ x_{target} - x_{cal}, y_{jet} + y_{target} - y_{cal}), which will nominally align the target with jetted drops (**Fig. 7d**).

The COM of object images are measured with standard Matrox image processing functions, including: i. capture the frame as an 8-bit grayscale image; ii. convert it to a black and white image using intensity thresholding; iii. perform blob analysis[17]; and iv. find the COM of the minimum bounding box of the splat blob.

Since the calibration splat and targets are so small, this strategy requires first moving these objects into the camera's field of view (FOV) at low magnifications (in Steps II and III) to facilitate searching for these objects as the tables are moved. Once in the FOV, they are moved into the approximate center of their respective images and then the camera magnification is increased. Since the zoom lens in the current system is manual, these steps are not fully automated. Therefore, the operator uses joystick control to first move the calibration splat into the camera's FOV at low magnification, centers it approximately in the image, and then the operator increases the magnification. The computer vision system (or the operator) draws a static cross-hair graphic through the COM_{cal} (Step II) as a visual guide for the next step. The operator then uses the joystick to move the target into the FOV at low magnification, and then centers the target under the cross-hair at high magnification (Step III). In a fully automated system, the cross-hairs would not be required, but only needed for visual verification by the operator. A variation of Step III is to move the target anywhere within the camera's FOV, measure the pixel offset between the target and COG_{cal}, convert this offset into an x-y distance using a known pixel/distance scale factor, and then add these distances to the equation in Step IV.

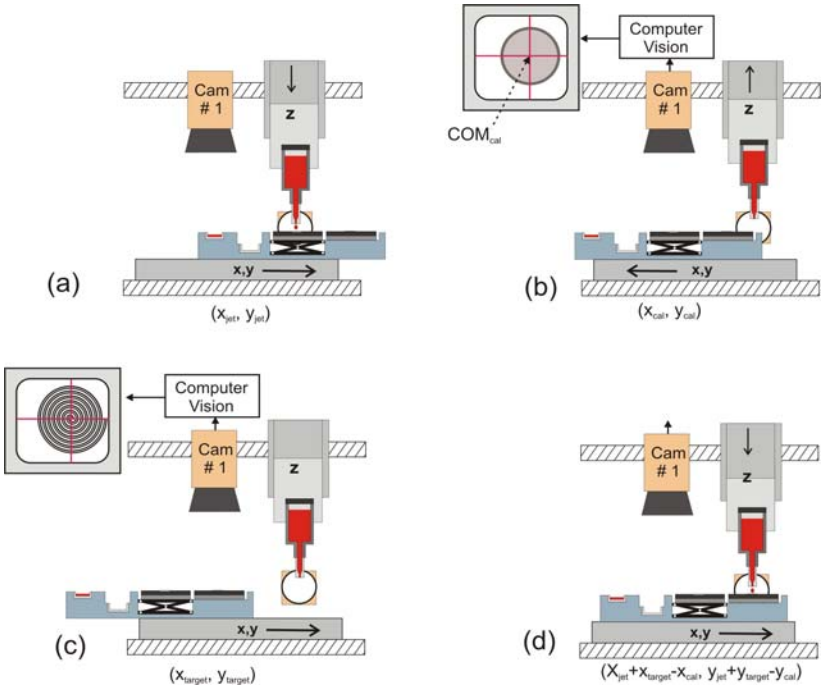

Figure 7. Targeting calibration steps.

Compensation for rotational misalignments. To deposit onto a chip with an array of transducer targets, the aforementioned calibration drop procedure need only be performed for one of the

targets since the relative positions between each transducer on a chip is known with high accuracy from the mask layouts used to fabricate the chips. However, the X-Y coordinates of the chip are not guaranteed to be in precise alignment with the X-Y coordinates of the servo stages. Therefore, in order to move the chip by a specified x-y distance relative to the calibrated target position, any rotational misalignment (ϕ) must be accounted for. Thus, an additional calibration step is required to determine the rotational matrix **M** that relates chip coordinates (x_{chip}, y_{chip}) to servo table coordinates (x_{table}, y_{table}):

$$\mathbf{M} = \begin{bmatrix} \cos\phi & -\sin\phi \\ \sin\phi & \cos\phi \end{bmatrix}$$

where

$$x_{table} = x_{chip}\cos\phi - y_{chip}\sin\phi \quad \textbf{Eq. 1}$$

$$y_{table} = x_{chip}\sin\phi + y_{chip}\cos\phi \quad \textbf{Eq. 2}$$

To determine ϕ, we move a second target on the array under the cross-hair and record the table positions ($x_{target\text{-}2}$, $y_{target\text{-}2}$) at that location. **Eqs. 1 and 2** can then be solved for ϕ*:*

$$\phi = \cos^{-1}[(\Delta x_{table}\Delta x_{chip}+\Delta x_{table}\Delta x_{chip})/(\Delta x^2_{chip}+\Delta y^2_{chip})] \quad \textbf{Eq. 3}$$

where

$(\Delta x_{table}, \Delta y_{table}) = (x_{target\text{-}2} - x_{target}, y_{target\text{-}2} - y_{target})$;

(x_{target}, y_{target}) are determined in Step III above; and

$(\Delta x_{chip}, \Delta y_{chip})$ are known distances in chip coordinates between the second target and first target.

Therefore, for an arbitrary target with a known displacement (δx_{chip}, δy_{chip}) from the first target, the change in table coordinates (δx_{table}, δy_{table}) from the original jetting position in Step IV is:

$$\delta x_{table} = \delta x_{chip}\cos\phi - \delta y_{chip}\sin\phi \quad \textbf{Eq. 4}$$

$$\delta y_{table} = \delta x_{chip}\sins\phi + \delta y_{chip}\cos\phi \quad \textbf{Eq. 5}$$

and, therefore jetting position to hit the arbitrary target is:

$$x_{table} = x_{jet} + x_{target} - x_{cal} + \delta x_{table} \quad \textbf{Eq. 6}$$

$$x_{table} = x_{jet} + x_{target} - x_{cal} + \delta x_{table} \quad \textbf{Eq. 7}$$

Repeatability: The polymer-based inks are dissolved and jetted in highly volatile organic solvents; therefore the viscosity of the ink in the jet nozzle is constantly changing (since it is exposed to air). One manifestation is that the first drop is jetting sequence will be slightly different in size than the subsequent drops. Drops size and viscosity variations can cause

significant device-to-device variations in quantity and morphology of deposited polymer (for the same deposition parameters).. These variations are also observed for bioprinting with the aqueous-based inks. We address this problem by incorporating a 'mini maintenance' operation between jettings onto each new device, or each line of a bio-array, whereby we first jet a few drops off to the side of the target, and then quickly move back to and jet onto the target location.

Jet Cleaning.

i. Polymers: After a jetting session is completed, all traces of polymer must be removed from the inkjet and reservoir. If polymer is not removed, cross contamination of polymer on future tests and nozzle clogging from dried polymer debris can occur. Polymer removal is accomplished by initially purging all polymer/solvent from the system using low positive pressure of 770 Torr. Residual polymer ink is then removed by successive flushes of clean toluene through the system. Approximately 200 μl of solvent is drawn into the inkjet through the nozzle, tubing and into the reservoir using negative pressure and then purged through the nozzle with positive pressure. Progress of the cleaning can be verified by the amount of polymer removed by the flushing operation during the purge cycle. A minimum of three flushes is generally required to yield a clear flush during the purge. After the clear solvent flush is obtained, additional solvent (50 μl) is drawn up into the reservoir using negative pressure. The final cleaning step is performed to verify that the inkjet and Teflon tubing is flushed with clean solvent. The reservoir is then removed from the inkjet and flushed independently with solvent.

ii. Growth Factors: After completing a bioink printing session, the nozzle is filled via vacuum and purged with positive pressure two times with 50 □l of 0.45 μm filtered distilled deionized water. 50 μl of 0.45 μm filtered 10% bleach is then drawn up into the jet and reservoir and allowed to remain in the jetting system for approximately ten minutes. The bleach is then purged from the jet and reservoir using positive pressure. The jet and reservoir are then extensively rinsed with filtered distilled deionized water prior to storage of the inkjet.

Software. With the exception of those operations requiring joystick control (as noted above), all operations are automatically controlled using custom software written in an interpreted, low-level Aerotech command language. Trigger commands are sent from the Aerotech controller to the JetDrive III controller to coordinate jetting with table motion.

JETTING ACCURACY

The accuracy of drop placement onto specified targets depends on several factors including: jet stability, random drop-to-drop trajectory deviations, stand-off distance between the jet and target substrates, as well as the target surface topology as described above. To characterize the inherent targeting accuracy of the system and removing surface topology as a variable, accuracy studies were conducted by depositing onto non-patterned plain silicon dioxide substrates. 'Virtual targets' were defined at arbitrary locations under the stationary cross-hair (Step III. in Targeting Calibration section). The specific steps for measuring accuracy were the same as the calibration steps described in the Targeting Calibration section, with the exception that the imaged COMs were also recorded for both the calibration drop and deposited target splat. The radial deviation of the COMs, converted from pixels to micrometers, defines the targeting accuracy. The pixels to μm conversion factor, which is 0.482 μm/pixel at 725X magnification,

was determined by imaging a 200 line/mm Ronchi ruling (Edmund Optics Inc., Barrington, NJ) and using Matrox imaging software to determine the number of pixels in the known distance.

Accuracy tests were conducted by depositing 4 x 6 arrays of 5mg/mil P3HT in TCB onto virtual targets, and repeated for different stand-off distances including 180, 400, and 800 μm. The target and calibration substrates were silicon wafers coated with 1μm SiO2. Two drops of P3HT polymer are initially deposited on the silicon calibration chip. The results are shown in **Table 1.**

Stand-Off Height (μm)	**Average offset** (μm)	**Std. Deviation** (μm)
180	3.9	2.7
400	9.9	2.7
880	21.3	4.0

Table 1. Targeting accuracy.

ACKNOWLEDGMENTS

This work was supported by AFOSR MURI F49620-02-1-0359, NIOSH-CDC 200-2002-00528, the National Science Foundation (Grants No. CTS-0210238 and DMI-9800565), the National Institutes of Health (Grant No. 1 R01 EB00 364-01), the Pennsylvania Infrastructure Technology Alliance (PITA) from the Pennsylvania Department of Community and Economic Development, and the Philip and Marsha Dowd Engineering Seed Fund. (The findings and conclusions in this report are those of the authors and do not necessarily represent the views of the National Institute for Occupational Safety and Health.)

References

1. Bedair, S.S.a.F., G. *CMOS MEMS oscillator for gas chemical detetcion*. in *Proc. IEEE Sensors Conf.* 2004. Vienna, Austria.
2. Sheats, J.R., *Manufactruing and commercialization issues in organic electronics.* J. Mater. Res., 2004. **19**(7): p. 1974-1989.
3. Shtein, M., Peumans, P., Benziger, J.B., and Forrest, S.R., *Direct, Mask- and Solevent-Free Printing of Molecular Organic Semiconductors.* Advanced Materials, 2004. **16**(18): p. 1615-1620.
4. Bietsch, A., Zhang, J., Hegner, M., Lang, H.P., and Gerber, C., *Rapid functionalization of cantilver array sensors ny inkjet printing.* Nanotechnology, 2004. **15**: p. 873-880.
5. Hayes, D.J., Cooley, P., and Wallace, D.B. *Miniature chemical and biomolecular sensors enabled by direct-write microdispensing technology*. in *SPIE Defense and Security Symposium*. 2004. Orlanod, FLA.
6. Service, R.F., *Printable Electronics That Stick Around.* Science, 2004. **304**: p. 675.
7. Sirringhaus, H., Kawase, T., Friend, R.H., Wu, W., and Woo, E.P., *High-Resolution Injet Printing of All-Polymer Transister Circuits.* Science, 2000. **290**(2123-2126).

8. Hierlemann A., B.O., Hagleitner C., and Baltes H., *Microfabrication Techniques for Chemical/Biosensors.* Proceedings of the IEEE, 2003. **91**(6): p. 839-863.
9. Wilson, T.S., Clarey, M., Stefan, P., Brown, S.B., Alvis, R.M., McBride, M.T., Langry, K., Maitland, D.J., and Colston, B.W. *MiDAS (Micro-dot Array Sensor): toward a rapid, in-vivo, reproducible, multianalyte biosensor using inkjet printing technology*. in *Lasers and Electro-Optics Society, 2002. LEOS 2002. The 15th Annual Meeting of the IEEE*. 2002.
10. Patel, S.V., T.E. Mlsna, B. Fruhberger, E. Klaassen, S. Cemalovoc, and D.R. Baselt, *Chemicapacitive microsensors for volatile organic compound detection.* Sensors and Actuators B, 2003. **96**(3): p. 541-553.
11. Campbell, P., E. Miller, L. Walker, G. Fisher, and L. Weiss, *Engineered Spatial Patterns of FGF-2 Immobilized on Fibrin Direct Cell Organization.* Biomaterials, 2005. **26**(33): p. 6762-6770.
12. Miller, E.D., G.W. Fisher, L.E. Weiss, L. Walker, and P. Campbell, *Dose-Dependent Cell Growth in Response to Concentration Modulated Patterns of FGF-2 Printed on Fibrin.* Biomaterials, 2005. **27**(10): p. 2213-2221.
13. Lee, E.R., *Microdrop Generation*. 2002: CRC Press.
14. Hasenbein, R. *Ink Jet Modeling FOr Development of New High Performance Ink Jet*. in *IS&T NIP18 Conference*. 2002. San Diego, California.
15. Fromm, J.E., *Numerical Calculation of the fluid dynamics of drop-on-demand jets.* IBM J. Res. & Dev., 1984. **28**(3): p. 322-333.
16. *MJ-AB User's Manual*, Microfab Technologies, Inc. p. 9-12
17. Ballard, D.H., and Brown, C.H., *Computer Vision*. 1982: Prentice-Hall.